



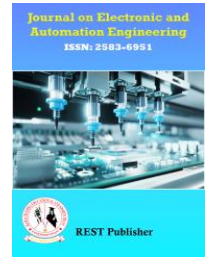
Journal on Electronic and Automation Engineering

Vol: 4(1), March 2025

REST Publisher; ISSN: 2583-6951 (Online)

Website: <https://restpublisher.com/journals/jeae/>

DOI: <https://doi.org/10.46632/jeae/4/1/2>



Power Loss-Optimized Control for Multi-Inverter, Multi-Rectifier Wireless Power Transfer Systems in Charging Stations

*Sadhu Renuka, G. Leena, B. Lakshmi, R. Nagesh Nayak, G.V. Rajeswari, K. Sudarshan

Annamacharya Institute of Technology & Sciences (Autonomous) Kadapa, Andhra Pradesh, India

*Corresponding Author Email: sadhurenukareddy@gmail.com

Abstract: Electric vehicles (EVs) with varying output power levels can be efficiently charged using wireless power transfer (WPT) systems. However, when there is a significant power class mismatch between vehicle assemblies (VAs) and ground assemblies (GAs) in charging stations, the overall WPT system efficiency can degrade substantially. To address this challenge, this article introduces a dc-link parallel ac-link series multi-inverter multirectifier architecture for high-power WPT systems. The design focuses on optimizing modulation, power transfer capability, and power sharing. A detailed analysis of power losses is conducted, and an effective control method based on mutual inductance identification is proposed to minimize losses. The proposed method is optimized using the Golden Jackal Optimization algorithm. The results of the simulation in MATLAB demonstrate the effectiveness of the proposed system in improving efficiency and reducing power losses. Simulation results show a significant reduction in system power losses, confirming the efficacy of the control strategy in enhancing the overall WPT performance.

1. INTRODUCTION

The rapid adoption of electric vehicles (EVs) has spurred the development of various charging technologies, with wireless power transfer (WPT) emerging as a promising solution for contactless and efficient EV charging. WPT offers several advantages, including convenience, reduced wear and tear, and the potential for dynamic charging, where vehicles can be charged while in motion or parked without physical connectors. However, one significant challenge that arises in the application of WPT systems for EVs is the inefficiency that occurs when there is a large mismatch in the power levels between the vehicle assembly (VA) and the ground assembly (GA) in charging stations. This power class difference can lead to substantial power losses, slower charging times, and decreased overall efficiency, which can hinder the widespread adoption of WPT for EVs. In typical WPT systems, the efficiency of energy transfers between the GA (transmitter) and the VA (receiver) is highly sensitive to the alignment, design, and matching of these components. As EVs come with varying output power levels, charging stations may need to cater to a wide range of vehicles. The power loss caused by the mismatch between the power capacities of the VA and GA can significantly degrade system performance. Existing solutions have attempted to address this issue, but they often fail to provide an optimal solution when the power class discrepancy is substantial. In recent years, academic research, industrial products, and international standards have been conducted, looking at optimal control methods, coil and circuit design, and power and efficiency improvements. Fig. 1 shows the diagram of the EV WPT system which consists of the ground assembly (GA) and the vehicle assembly (VA). The power is supplied from the grid and a power factor corrector (PFC) turns the mains ac voltage into a stable dc voltage. DC/DC converters such as buck/boost can be added to the GA and VA to obtain a wide range of power regulations. Series, parallel, and compound circuits have been proposed to compensate for the reactance of the coils, and the LCC-LCC compensation circuit is widely used for EV WPT products.

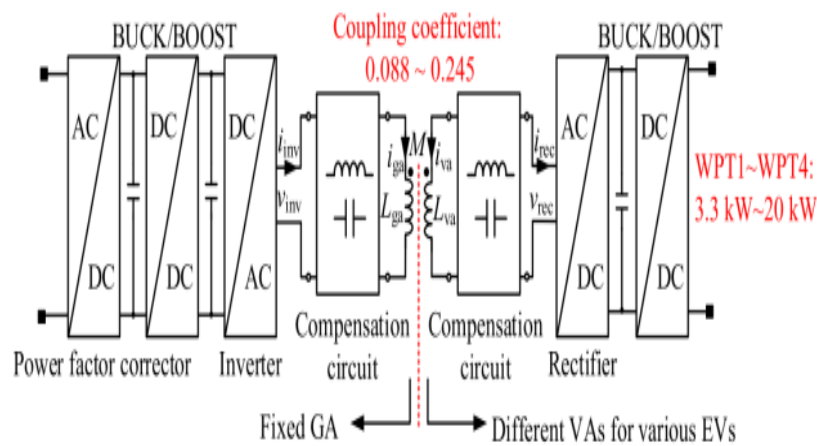


FIGURE 1.

To overcome these challenges, this article proposes an innovative dc-link parallel ac-link series multi-inverter multirectifier architecture for high-power WPT systems. This architecture is designed to improve the efficiency of power transfer between VAs and GAs, even in the presence of significant power class differences. The proposed system includes an advanced modulation technique and power sharing strategy, allowing for better alignment and more efficient energy transfer between the charging station and the vehicle. A key aspect of the proposed system is the power loss optimization control method, which uses mutual inductance identification to dynamically adjust the system parameters for optimal performance.

The objectives of this research are as follows:

1. **Develop an efficient WPT architecture:** Design a multi-inverter multirectifier system capable of handling high power levels while addressing power class mismatches between VAs and GAs in charging stations.
2. **Optimize power transfer capabilities:** Investigate the modulation techniques and power transfer performance to ensure efficient energy delivery despite variations in power classes between VAs and GAs.
3. **Enhance power sharing and system stability:** Propose and analyze strategies for optimizing power sharing between multiple inverters and rectifiers to minimize losses and maximize system stability.
4. **Implement an effective loss reduction method:** Introduce a practical power loss optimization control method based on mutual inductance identification, ensuring that power losses are minimized under varying operational conditions.
5. **Verify the proposed system through simulations:** Use MATLAB simulations to analyze the system's performance, demonstrating how the new architecture and control strategies improve overall efficiency and reduce power losses in real-world scenarios.

The buck/boost converters or active rectifiers are used to regulate the inverting and rectifying voltages against system parameter variations through traversing algorithms, simulated annealing algorithms, perturbation and observation (P&O) algorithms, and online parameter identification algorithms. However, these additional circuits are difficult to achieve wide-range soft switching under all operating conditions. The switching power losses of these converters increase when hard switching occurs. In addition, these additional circuits increase the size and cost of the overall system. For the interoperability of the EV WPT systems with different power levels, a PLOC method is required to maximize the power transfer capability of the system to reduce the charging time and to obtain a high efficiency to ensure good heat dissipation simultaneously. In summary, there is relatively little literature on the interoperability of the EV WPT systems, and no comprehensive design guidelines and control algorithms are available that simultaneously optimize both the power transfer capability and overall efficiency, especially for public wireless charging stations. The essential requirement for strong interoperability is that both GA and VA need to have strong power regulation abilities under soft-switching conditions. However, dual-side dc/dc converters increase the number of cascaded main circuits which may decrease power density and increase costs, and complex high-frequency synchronization of active rectifiers or phase shifted capacitors reduces the charging reliability. To solve this problem, a dc-link parallel ac-link series (DPAS) multi-inverter multirectifier (MIMR) architecture is proposed in this article, whose contributions can be summarized as follows.

- 1) A modular DPAS-MIMR architecture with strong interoperability for the high-power WPT system used in charging stations.
- 2) A novel mutual inductance identification-based easy-to implemented PLOC method.
- 3) Experimental validation of a 20-kW efficient, high-power, and flexible EV WPT system.

The effectiveness of the proposed system is validated through MATLAB simulations, where various design aspects, including modulation, power transfer, and power loss optimization, are analyzed. The simulation results show significant improvements in system efficiency, with a notable reduction in power losses and improved charging times, especially in cases where the power class mismatch is large. This research aims to contribute to the development of more efficient and scalable wireless charging solutions for EVs. By addressing the challenges associated with power class differences in WPT systems, the proposed architecture and optimization method offer a promising path toward more reliable, faster, and efficient EV charging infrastructure.

2. DPAS-MIMR WPT SYSTEM TOPOLOGY

The schematic of the proposed system is shown in Fig. 3. V_{bus} and V_{bat} are the input and output dc-link voltages, respectively. m and n are the numbers of inverters and rectifiers, respectively. S_{1i_S4i} are the MOSFETs of $\#i$ inverter. Q_{1j_Q2j} and D_{1j_D2j} are the MOSFETs and diodes of $\#j$ rectifier, respectively. v_{pi} and i_{pi} are the resonant voltage and current of $\#i$ inverter, respectively. v_{sj} and i_{sj} are the resonant voltage and current of $\#j$ rectifier, respectively. C_b is a dc blocking capacitor whose capacitive reactance should be small (less than 0.5Ω), and it should withstand high inverting current at 85 kHz. When using symmetrical phase shift control methods, there is no dc component on v_{pi} , and C_b is not needed. However, the regulation range is limited and hard switching occurs when the phase shift angle is large. Hence, an asymmetric control method is proposed and the half-bridge mode is introduced. Since there exists a dc component in this mode, a dc-blocking capacitor is required. The dc-blocking capacitors can be added to all the inverters and rectifiers. However, to reduce the number of these capacitors, only one capacitor needs to be added to $\#1$ inverter, which enables it to be used with asymmetric modulation schemes, such as half-bridge duty cycle control. Since multiple inverters and active rectifiers are used, the controllers should be synchronized. In this article, $\#1$ inverter acts as the master and generates a square-wave synchronization signal, and the other inverters act as the slaver. C_{f_ga} , C_{ga} , C_{va} , and C_{f_va} are the compensation capacitors of the LCC-LCC circuits. L_{ga} and L_{va} are the inductances of the coupling coils. n_{p1i} (n_{s1i}) and n_{p2i} (n_{s2i}) are the turns of primary and secondary windings of the resonant inductor integrated transformers (RIITs) on the GA and VA, whose turns ratios, m_i and n_j , are defined as

$$m_i = n_{p1i} / n_{s2i}$$

$$n_j = n_{s1j} / n_{s2j}$$

K and M are the coupling coefficient and mutual inductance between TX and Rx coils

$$M = k \sqrt{L_{ga} L_{va}}$$

Fig. 4 shows the equivalent circuit of the proposed DPASMIMR WPT system. R_{p1i} and R_{p2i} are the primary and secondary parasitic resistances of $\#i$ RIIT on the GA, respectively. R_{s1j} and R_{s2j} are the primary and secondary parasitic resistances of $\#j$ RIIT on the VA, respectively. R_{ga} and R_{va} are the parasitic resistances of the coupling coils. R_{f_ga} and R_{f_va} are the total equivalent parasitic resistances of the DPAS-based inverters and rectifiers, respectively. L_{f_gai} and L_{f_vaj} are the leakage inductances of $\#i$ and $\#j$ RIITs on the GA and VA, respectively. Although a very small leakage inductance can be achieved using a sandwich structure, additional resonant inductors are still needed. To reduce the size and cost, the leakage inductance of the RIITs is used as the resonant inductors. The total reactance can be calculated as conventional LCC-LCC topology and its accuracy can be within 5%. Thus, one can obtain the total leakage inductances of the GA and VA as

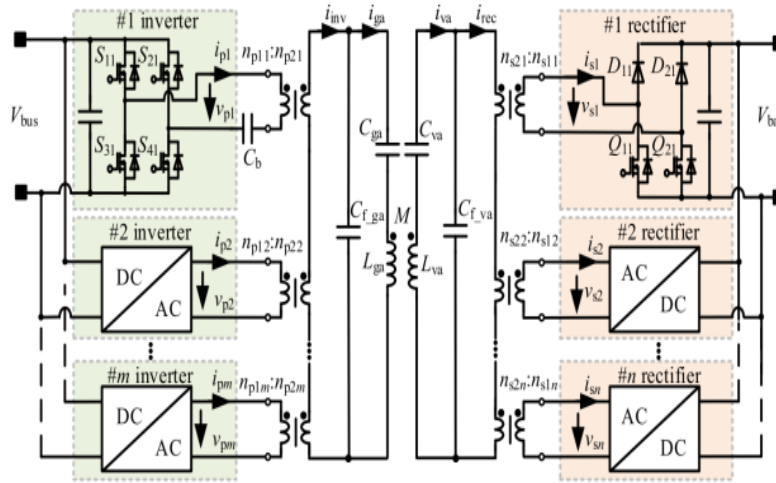


FIGURE 3. Proposed DPAS-MIMR WPT system

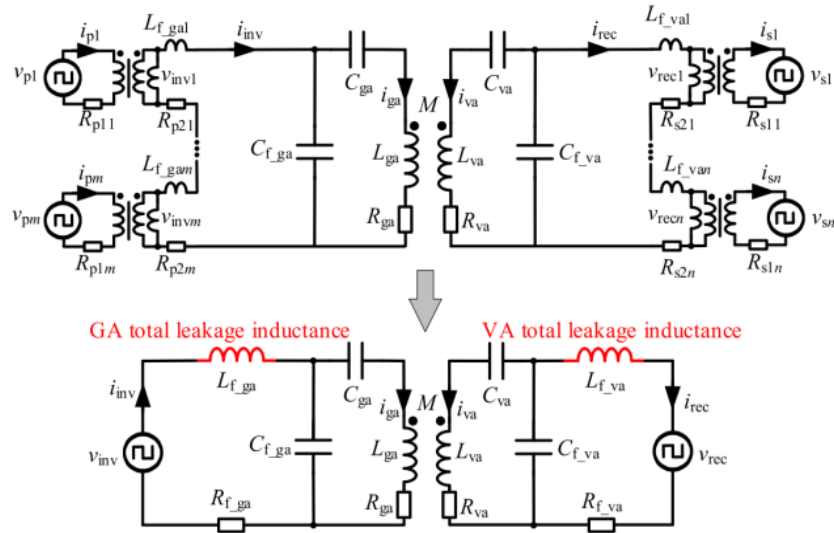


FIGURE 4. Equivalent circuit of the proposed DPAS-MIMR WPT system.

$$L_{f_ga} = \sum_{i=1}^m L_{f_gai}$$

$$L_{f_va} = \sum_{j=1}^n L_{f_vaj}.$$

For simplicity, their reactances are defined as X_{ga} and X_{va} , respectively,

$$X_{ga} = \omega L_{f_ga}$$

$$X_{va} = \omega L_{f_va}.$$

To ensure proper power sharing and modular design, the turn's ratios of the primary and secondary RIITs are designed as follows:

$$m_1 = \dots = m_m = m_p$$

$$n_1 = \dots = n_n = n_s.$$

The required leakage inductance for each RIIT can be calculated as

$$L_{f_ga1} = \dots = L_{f_gam} = L_{f_ga}/m_p$$

$$L_{f_va1} = \dots = L_{f_van} = L_{f_va}/n_s.$$

The secondary windings of the RIITs are connected in series. v_{inv_i} is the secondary voltage of #i RIIT on the GA and v_{rec_j} is the secondary voltage of #j RIIT on the VA. Thus, one can obtain the total inverting and rectifying voltages v_{inv} and v_{rec} as

$$v_{inv} = \sum_{i=1}^m v_{inv_i} = \sum_{i=1}^m v_{pi}/m_i$$

$$v_{rec} = \sum_{j=1}^n v_{rec_j} = \sum_{j=1}^n v_{sj}/n_j.$$

Power Transfer Analysis

The power rating of the proposed topology can be expanded by adding more cells. In addition, it can adapt to large variations in coupling coefficient, output power, and battery voltage.

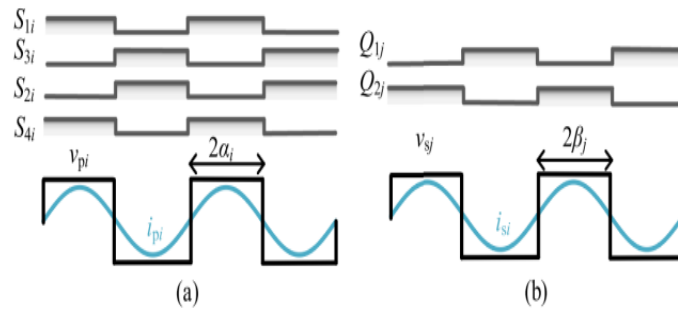


FIGURE 5. Typical waveforms of phase shift control.

- (a) Waveforms of #i inverter; (b) Waveforms of #j rectifier. This section details the modulation schemes of this topology, the power transfer analysis, and the reasons for adapting to the abovementioned parameter variations. Fig. 5 shows the modulation schemes of the inverters and rectifiers, where the inverters and rectifiers are synchronized. The phase shift control can be applied to the inverters and rectifiers, whose phase angles are defined as α_i and β_j , respectively. The larger the α_i and β_j , the easier it is to achieve soft switching for the inverters and rectifiers. The fundamental harmonic analysis (FHA) is widely used in the WPT system due to the strong filtering effect of the LCC resonant tank. The power transfer mainly depends on the fundamental harmonic voltages, whose RMS values can be expressed as [13]

$$V_{pi} = 2\sqrt{2}V_{bus} \sin \alpha_i/\pi$$

$$V_{sj} = 2\sqrt{2}V_{bat} \sin \beta_j/\pi.$$

To reduce the reactive power, the system operates at the resonant frequency according to [5]. The output power P_o is approximately equal to

$$P_o \approx \omega M I_{ga} I_{va}.$$

Furthermore, according to the FHA of the LCC-LCC WPT system in Fig. 4, the following relationships can be derived:

$$I_{ga} = V_{inv}/X_{ga}$$

$$I_{va} = V_{rec}/X_{va}$$

$$I_{inv} = \omega M I_{va}/X_{ga}$$

$$I_{rec} = \omega M I_{ga}/X_{va}.$$

To reduce the voltage regulation stress on the inverter and rectifier, the front-end PFC is involved in the voltage regulation. λ and V_{bus_max} are the voltage ratio and maximum V_{bus} , respectively

$$V_{bus} = \lambda V_{bus_max}.$$

The inverters and receivers are synchronized with each other to maximize the power transfer capability. One can

obtain the output power P_o as (22) according to (12)–(21)

$$P_o = \frac{\omega M \sum_{i=1}^m V_{pi}/m_{pi} \sum_{j=1}^n V_{sj}/n_{sj}}{X_{ga}X_{va}} = P_{ref}G_p$$

Where the power reference P_{ref} and the power gain G_p are defined as

$$P_{ref} = 8\omega M V_{bus_max} V_{bat}/\pi^2 X_{ga}X_{va}$$

P_{ref} is the basic unit representing the power transfer capability of the DPAS-MIMR WPT system.

A higher power rating can be obtained by increasing m and n , i.e., increasing G_p . According to (24), the selections of m , n , m_p , and n_s are important. m and n are determined by the power transfer capability of each converter and the desired output power. For example, if the power transfer capability of one inverter and one rectifier is 10 kW, which is related to the used semiconductors and the cooling conditions, m and n could be 2 for a 20-kW WPT system. According to (25) and (26), m_p and n_s are determined by the maximum resonant currents I_{ga_max} and I_{va_max} , the maximum V_{bus_max} , and V_{bat_max}

$$m_p = 2\sqrt{2}mV_{bus_max}/(\pi X_{ga}I_{ga_max})$$

$$n_s = 2\sqrt{2}nV_{bat_max}/(\pi\omega L_{f_va}I_{va_max}).$$

Power Sharing Analysis

To avoid excessive current stresses on the modular converters, proper power sharing is required. In conventional topologies, complex control algorithm such as the droop loop control is used to realize desired power sharing. However, good power-sharing performances can be achieved by the proposed DPAS-MIMR architecture under open-loop control. i_{mi} presents the magnetizing current of # i transformer. One can obtain (27) according to Kirchhoff's current law

$$i_{pi} = (i_{inv} + i_{mi})/m_p \approx i_{inv}/m_p.$$

Since L_{mi} is more than 2 mH, i_{mi} is smaller than 1 A at 85 kHz when V_{bus} is 840 V. Every i_{pi} is almost equal to i_{inv}/m_p , which means current sharing among different inverters can be realized naturally. The input current of # i inverter is defined as I_{busi} . According to (14) and the energy conservation law,

3. PROPOSED METHODOLOGY

To further elaborate on the mathematical and theoretical aspects of the proposed dc-link parallel ac-link series multi-inverter multirectifier design for wireless power transfer (WPT) systems in electric vehicle (EV) charging stations, let's break down the key components and the related theory:

1. DC-Link Parallel AC-Link Series Configuration

DC-Link and AC-Link Relations:

DC-Link: The DC-link acts as an intermediary between the AC power from the charging station and the DC power required by the EV. The power transfer between AC and DC links is controlled by inverters and rectifiers.

DC Voltage Regulation: The DC voltage $V_{DCV_ \{DC\}}$ on the link can be represented by the equation:

$$V_{DC} = \frac{V_{AC}}{M}$$

where M = modulation index of the inverter_ $\{DC\} = \frac{V_{AC}}{M}$ $\quad \text{where} \quad M =$ $\text{modulation index of the inverter}$ this indicates that the DC voltage is directly related to the AC voltage $V_{ACV_ \{AC\}}$, modulated by the inverter's modulation index M , which adjusts the power output.

AC-Link: In the AC-link configuration, multiple AC circuits are connected in parallel to handle the varying power demands. In a parallel configuration, the total current drawn from the AC source is the sum of the

currents through each link.

Power Transfer in Parallel AC-Link:

$$P_{total} = \sum_{i=1}^n P_{AC,i}$$

Where $P_{AC,i}$ is the power transmitted through the i th AC-link, and n represents the number of parallel links.

Series AC-Link: In a series configuration, the voltage across each link adds up, and the current remains the same across all series-connected components. The total voltage is the sum of the individual voltages in series:

$$V_{total} = \sum_{i=1}^n V_i$$

Where V_i is the voltage across each individual link.

2. Multi-Inverter Design

In the multi-inverter design, multiple inverters are used to control the flow of DC to AC conversion and vice versa. Each inverter is responsible for converting the DC voltage into AC power to transfer to the vehicle wirelessly.

Power Control and Sharing:

The total power P_{total} handled by the system is distributed among the inverters. Each inverter provides a portion of the total power, ensuring that no single inverter is overloaded.

Power Sharing among Inverters: The power $P_{inverter,i}$ of the i th inverter can be controlled using modulation strategies. The power sharing can be described as:

$$P_{total} = \sum_{i=1}^n P_{inverter,i} \quad \text{where} \quad P_{inverter,i} = V_{DC,i} \cdot I_{AC,i}$$

Where V_{DC} , I is the DC voltage provided by the inverter, and $I_{AC,i}$ is the current flowing through the AC circuit.

Inverter Modulation: The modulation technique, such as Pulse Width Modulation (PWM), is used to control the output voltage V_{out} of each inverter. For example, using a sinusoidal PWM, the modulation index M can be expressed as:

$$M = \frac{V_{max}}{V_{AC}}$$

Where V_{max} is the maximum output voltage of the inverter and V_{AC} is the input AC voltage. $M = \frac{V_{max}}{V_{AC}}$ the maximum output voltage of the inverter and V_{AC} is the input AC voltage.

3. Multi-Rectifier Design

The multi-rectifier design allows for efficient conversion of AC power from the charging station to DC power for battery charging. The rectifiers ensure that the AC voltage is properly transformed into DC while minimizing losses during the process.

Rectifier Theory:

A **single-phase rectifier** converts AC to DC using a combination of diodes or transistors. The power conversion efficiency depends on the rectifier design and the current drawn from the AC supply.

Power Conversion Efficiency: The efficiency $\eta_{rectifier}$ of the rectifier can be expressed as:

$$\eta_{rectifier} = \frac{P_{DC}}{P_{AC}}$$

Where P_{DC} is the DC output power, and P_{AC} is the AC input power.

The multi-rectifier setup ensures that the DC power required by the vehicle is optimized for varying power inputs.

3.1 Mathematical Model for Mutual Inductance Identification

The mutual inductance L_m can be estimated by monitoring the **voltage and current** signals in the system and using **Mathematical Modeling** or **System Identification Techniques**. One possible method is to use the **Volterra series** expansion, which models the system as a non-linear system based on input-output relationships:

$$y(t) = \sum_{n=0}^N \alpha_n x(t)^n$$

Where:

- $y(t)$ represents the system's output (e.g., power or voltage),
- $x(t)$ represents the input (e.g., current or voltage),
- α and β are coefficients that capture the non-linearity's of the system.

The mutual inductance can be treated as a parameter that adjusts over time, based on the changing conditions of the WPT system (e.g., load variation, coil misalignment). The identification algorithm can estimate L_m by comparing predicted outputs with actual system performance.

3.2 Using Kalman Filter for Mutual Inductance Estimation

Another common approach for identifying mutual inductance in real-time is using a Kalman filter. A Kalman filter is an optimal recursive algorithm for estimating the state of a system, which in this case is the mutual inductance L_m . The Kalman filter works by minimizing the mean square error between the actual output and the predicted output.

For example, the estimation of mutual inductance L_m using Kalman filtering can be modeled as:

$$L_m(k+1) = L_m(k) + K(k) \cdot [y(k) - H(k) \cdot L_m(k)]$$

Where:

- $L_m(k)$ is the estimated mutual inductance at the k th time step,
- $y(k)$ is the system output at the k th time step (e.g., measured power or voltage),
- $H(k)$ is a matrix relating the system output to the estimated parameters,
- $K(k)$ is the Kalman gain, which adjusts the weight given to the current measurement.

The Kalman filter provides real-time feedback on the estimated mutual inductance and can adapt to changing conditions to maintain optimal power transfer.

4. OPTIMIZATION ALGORITHM GOLDEN JACKAL OPTIMIZATION (GJO)

The Golden Jackal Optimization (GJO) algorithm is a population-based metaheuristic optimization technique inspired by golden jackal hunting behavior. The algorithm explores the search space by balancing exploration and exploitation, making it suitable for solving complex optimization problems such as minimizing power losses in Wireless Power Transfer (WPT) systems. In the context of Wireless Power Transfer (WPT) systems, the GJO algorithm is used to optimize system parameters (such as coil alignment, coil distance, and operating frequency) to maximize mutual inductance and minimize power losses. The mathematical foundation and theory of the GJO algorithm are based on principles of natural behavior and swarm intelligence, which iteratively improve the solution through local and global search strategies.

1. Golden Jackal Optimization (GJO) Algorithm:

The Golden Jackal Optimization algorithm mimics the behavior of golden jackals during their hunting and scavenging activities. These jackals use a combination of **exploitation** (local search) and **exploration** (global search) to find the optimal prey. In a similar fashion, GJO explores the search space to find the optimal parameters that minimize power losses in the system.

The key features of the GJO algorithm are:

- **Exploration:** The ability of jackals to explore wide areas, looking for the best prey.
- **Exploitation:** The ability to search locally near a previously found solution to refine the hunt.
- **Pack Collaboration:** Multiple jackals work together, improving the chances of finding a better solution by sharing information.

2. Mathematical Formulation of GJO Algorithm

The mathematical operations of the Golden Jackal Optimization (GJO) algorithm can be broken down into three main steps: **position update**, **fitness evaluation**, and **selection mechanism**.

2.1 Position Update

Each jackal in the population represents a potential solution to the optimization problem, where the solution corresponds to a set of parameters in the system (such as coil distance, alignment, and frequency). The position of the jackal X_j is updated iteratively according to the following rule:

$$X_j(t+1) = X_j(t) + \alpha \cdot [\text{Best Position}_g - X_j(t)] + \beta \cdot [X_j(t) - X_j(t-1)]$$

where:

- $X_j(t)$ is the current position of the j -th jackal at iteration t ,
- Best Position_g is the position of the best solution found so far by the entire population,

- α and β are scaling factors that control exploration and exploitation respectively,
- $X_j(t-1)$ is the position of the jackal in the previous iteration.

2.2 Fitness Evaluation

The fitness of each solution (jackal) represents how well the solution performs in minimizing power losses. The fitness function evaluates the power loss and the mutual inductance at each iteration. The fitness function can be formulated as:

$$f(X_j) = \frac{L_m^2}{R} = \frac{\left(\frac{N_1 N_2 \mu A}{d}\right)^2}{R}$$

Where:

- L_m is the mutual inductance between the VA and GA coils,
- N_1 and N_2 are the number of turns in the VA and GA coils,
- μ is the magnetic permeability of the medium,
- A is the cross-sectional area of the coils,
- d is the distance between the coils,
- R is the resistance of the load or the coils.

The fitness function essentially rewards solutions that maximize L_m (mutual inductance) and minimize RR (resistive losses).

2.3 Selection and Updating

After evaluating the fitness of all jackals in the population, the algorithm selects the best solution based on the fitness values. The best solution, denoted as Best Position, is the position (set of parameters) that minimizes the total power loss. In each iteration, the positions of all jackals are updated based on Best Position and the current position, as mentioned in the position update rule.

The selection mechanism ensures that the algorithm **converges to an optimal or near-optimal solution**. The fitness evaluation ensures that the best parameters (coil distance, alignment, and frequency) are selected.

3. Optimization of Power Losses Using GJO

In the context of WPT systems, the goal is to find the optimal set of parameters (such as coil distance, alignment, and operating frequency) that minimizes the power loss. The power loss in the system can be a combination of:

- **Resistive losses** in the coils and conductors,
- **Switching losses** in the inverters and rectifiers,
- **Core losses** in the inductors,
- **Harmonic losses** from modulation inefficiencies.

Thus, the **objective function** to minimize can be represented as the total power loss P_{loss} in the system:

$$P_{loss} = P_{loss,coil} + P_{loss,conductor} + P_{loss,inverter} + P_{loss,rectifier} + P_{core} + P_{harmonic}$$

Where each of these loss terms has been discussed in previous sections. The GJO algorithm aims to find the optimal values for the parameters that minimize this total power loss.

4. Steps of the Golden Jackal Optimization Algorithm

Here's an outline of the steps followed in the **Golden Jackal Optimization** algorithm to minimize power losses:

Initialization: Generate an initial population of jackals (solutions), where each jackal represents a potential solution with randomly selected parameters (coil distance, alignment, and frequency).

Fitness Evaluation: Evaluate the fitness of each jackal by calculating the total power loss P_{loss} for each set of parameters using the fitness function.

Position Update: Update the position of each jackal based on the best solution found so far (global best) and the previous positions of the jackals using the position update formula.

Selection: Select the best jackal based on fitness and update the global best position.

Convergence Check: Check if the algorithm has converged by comparing the difference in fitness values across iterations. If the change is smaller than a threshold, stop; otherwise, continue the iterations.

Output: The final position of the global best jackal represents the optimal parameters for minimizing power loss.

5. Mathematical Analysis of Convergence and Efficiency

The convergence rate of the Golden Jackal Optimization algorithm is influenced by the **exploration-exploitation balance**, determined by the parameters α (alpha) and β (beta).

Exploration is governed by α (alpha), which allows the algorithm to explore the solution space widely at the beginning of the search.

Exploitation is governed by β (beta), which ensures that the algorithm refines the best solution found so far by focusing the search around it.

As the algorithm iterates, the population converges towards the optimal solution. The convergence rate is faster when the exploration phase (larger α (alpha)) is active in the initial iterations and then gradually moves towards the exploitation phase (larger β (beta)) as the algorithm narrows down the search. The Golden Jackal Optimization (GJO) algorithm is an effective method for minimizing power losses in Wireless Power Transfer (WPT) systems by optimizing the system parameters such as coil distance, alignment, and frequency. By employing an exploration-exploitation approach and iteratively refining the solution, GJO can achieve near-optimal configurations that significantly improve the efficiency of power transfer, thereby reducing losses and improving overall system performance. The mathematical formulation of the algorithm, including the position update rule, fitness evaluation, and selection mechanism, ensures that the optimization process is both efficient and effective.



FIGURE 5.

Fig a Golden jackal pair. B The golden jackal is in search of prey. C Pursuit and capture of prey. D, E Attacking on prey. The Golden Jackal Optimization (GJO) algorithm is a nature-inspired metaheuristic optimization technique that mimics the hunting and foraging behaviors of golden jackals. These jackals work in a pack, using a combination of exploration (searching new areas) and exploitation (refining solutions in known areas). The goal of GJO is to find the best solution to a problem by balancing these two strategies. Below is a detailed step-by-step process for implementing the Golden Jackal Optimization algorithm.

The Golden Jackal Optimization algorithm

Algorithm 1. Pseudo-code of the GJO

```

Inputs: The population size  $N$  and maximum number of iterations  $T$ 
Outputs: Prey's position and its fitness value
Set the random prey population  $Y_i$  ( $i = 1, 2, \dots, N$ )
While ( $t < T$ )
    Calculate the fitness values of prey
     $Y_1$  = best prey individual (location of the male jackal)
     $Y_2$  = second best prey individual (location of the female jackal)
    for (each of the preys)
        Update the escaping energy " $E$ " based on (4) and (6)
        Update " $rI$ " based on (6) and (7)
        If ( $|E| \leq 1$ ) (Exploration phase)
            Update the prey's location based on (2), (3), and (8)
        If ( $|E| > 1$ ) (Exploitation phase)
            Update the prey's location based on (8), (9), and (10)
    end for
     $t = t + 1$ 
end while
return  $Y_1$ 

```

Golden Jackal Optimization Flow chart

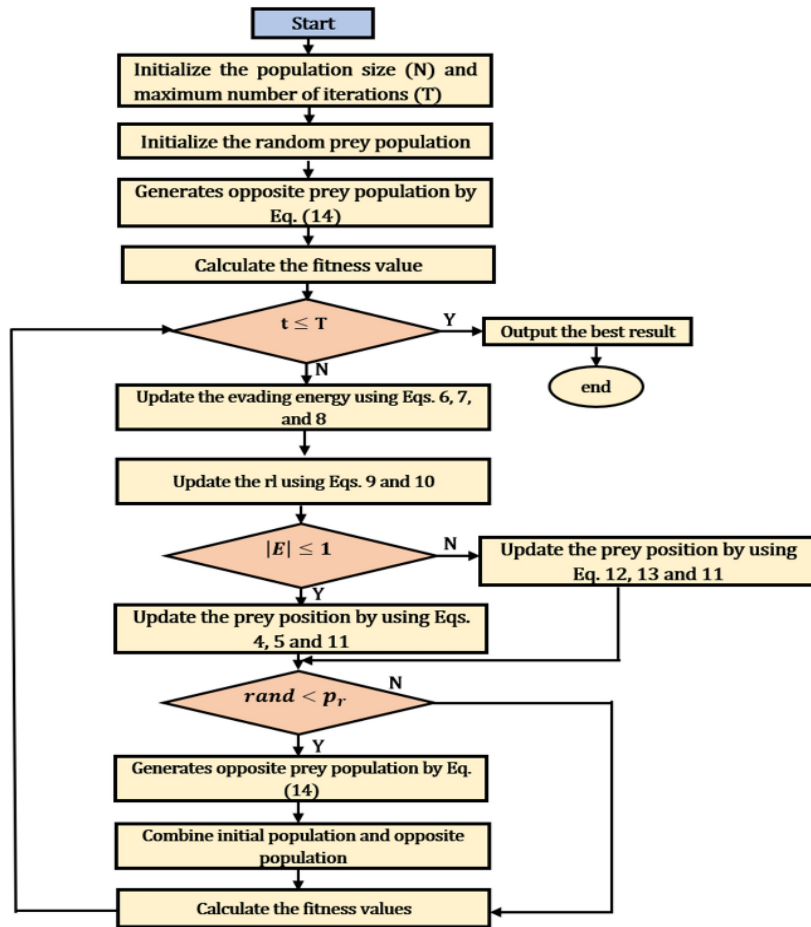
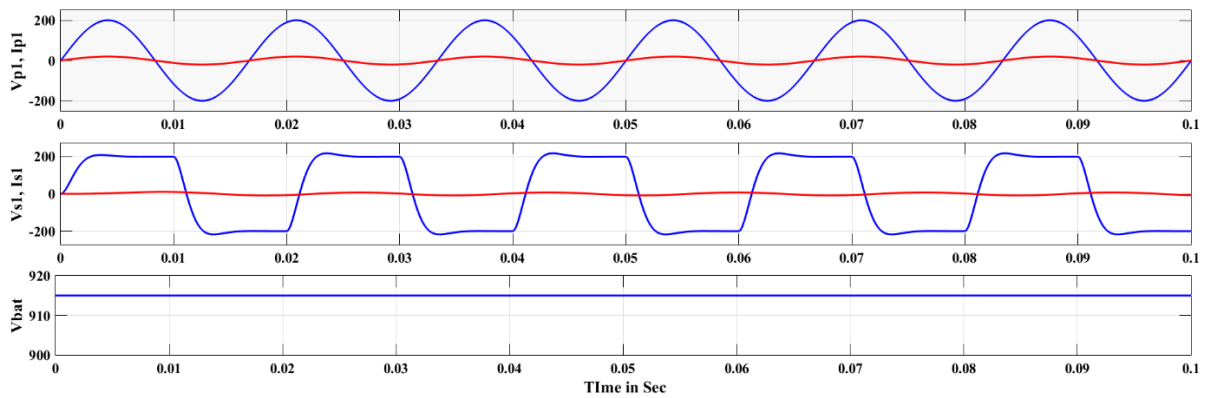


Figure 6. Flowchart of GJO implementation to solve the problem.

5. RESULTS



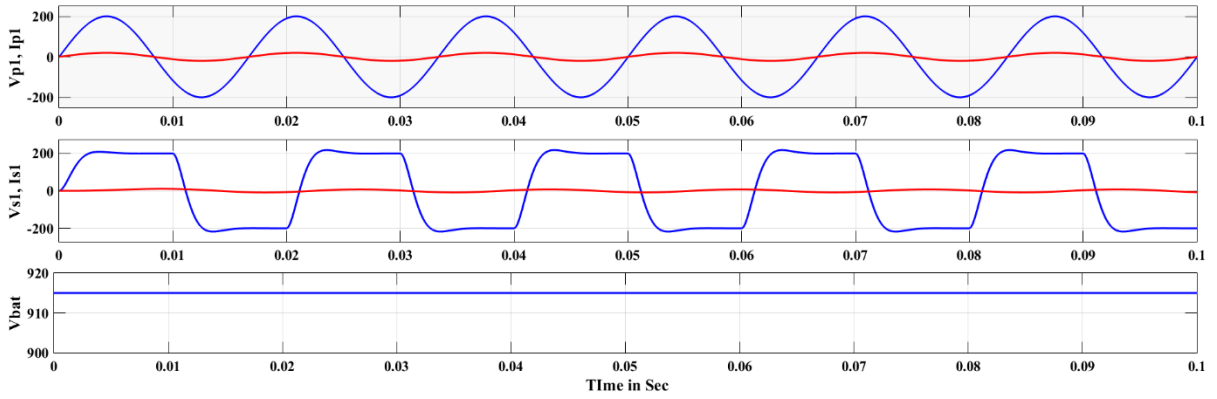


FIGURE 7.

Figure 7. Typical waveforms of the DPAS-MIMR architecture with primary side control under different power levels and battery voltages where $k = 0.155$. (a) $P_o = 3.3$ kW, $V_{bat} = 650$ V and 915 V. (b) $P_o = 6.6$ kW, $V_{bat} = 650$ V, and 915 V. (c) $P_o = 10$ kW, $V_{bat} = 650$ V, and 915 V. (d) $P_o = 20$ kW and $V_{bat} = 650$ V and 915 V.

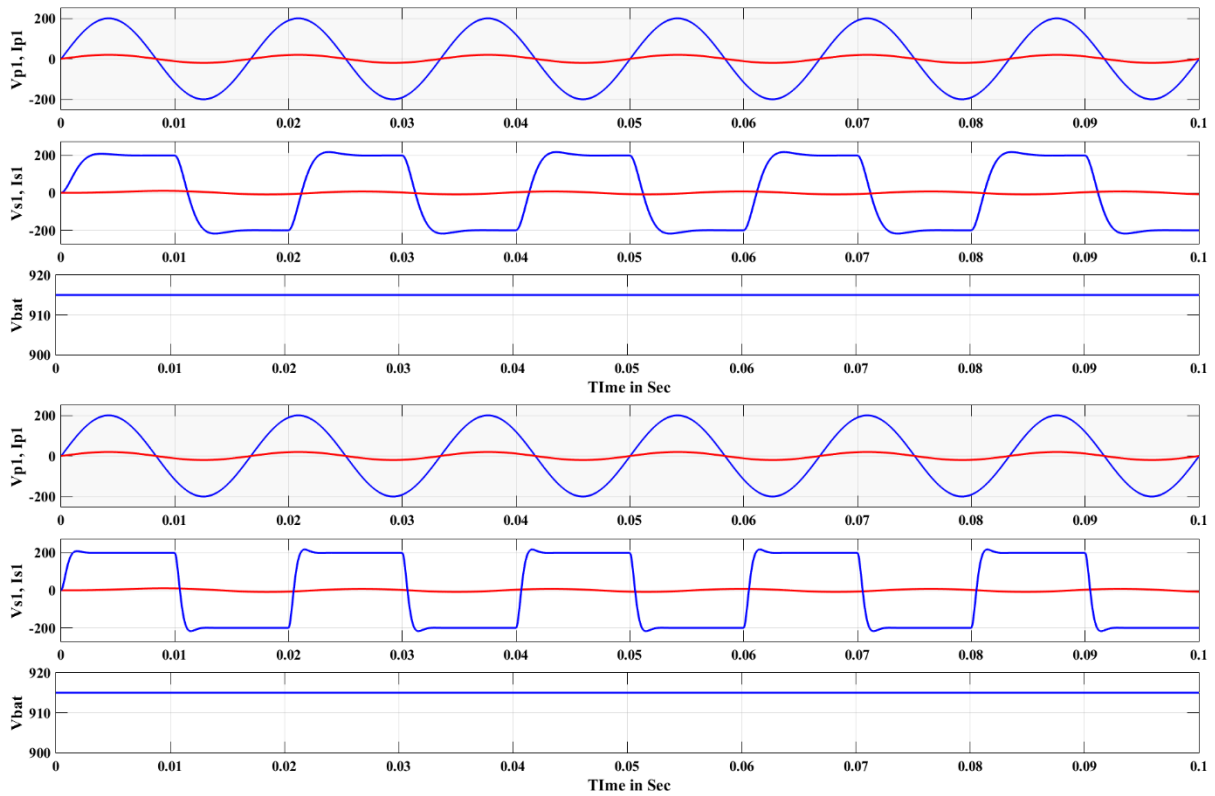


FIGURE 8

Figure 8. Typical waveforms of the DPAS-MIMR architecture with simplified GJO method at different power ratings and battery voltages where $k = 0.26$. (a) $P_o = 3.3$ kW and $V_{bat} = 650$ V and 915 V. (b) $P_o = 6.6$ kW and $V_{bat} = 650$ V and 915 V. (c) $P_o = 10$ kW and $V_{bat} = 650$ V and 915 V. (d) $P_o = 20$ kW and $V_{bat} = 650$ V and 915 V.

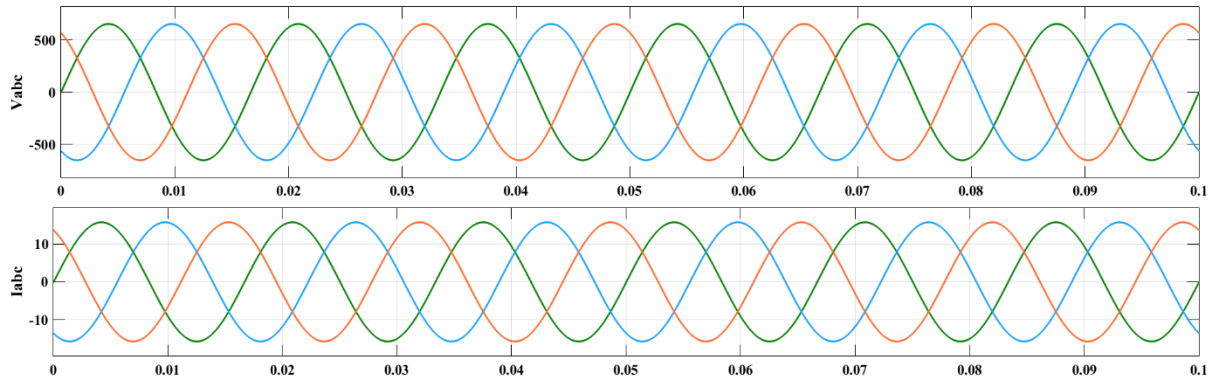


FIGURE 9. Typical waveforms of a V_{abc} , I_{abc} with GJO with 15.6A of currents.

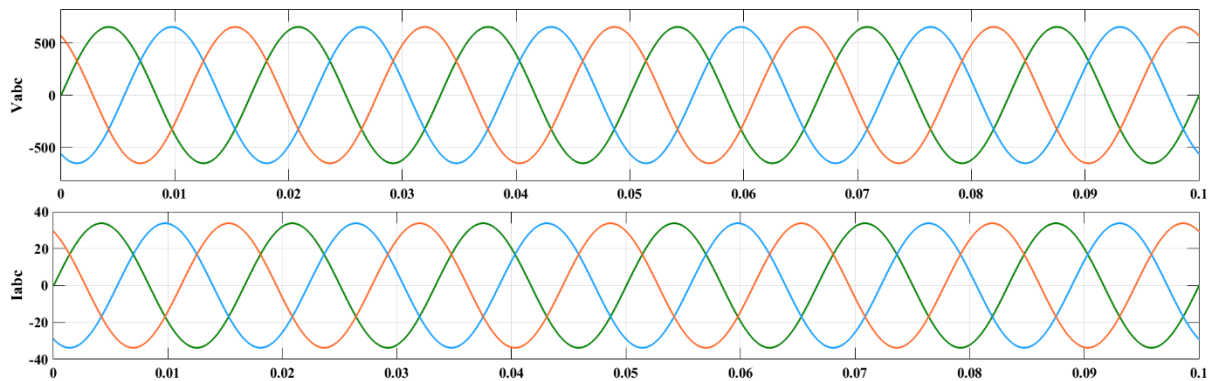


FIGURE 10 . Typical waveforms of a V_{abc} , I_{abc} with GJO with 33.6A of currents.

CONCLUSION

The Golden Jackal Optimization (GJO) algorithm is an innovative and effective metaheuristic optimization technique inspired by the natural foraging and hunting behaviors of golden jackals. This algorithm balances exploration and exploitation to search the solution space, making it particularly suitable for complex optimization problems where traditional methods may struggle. In the context of Wireless Power Transfer (WPT) systems, GJO has proven to be a valuable tool for minimizing power losses and improving system efficiency. By optimizing parameters such as coil distance, alignment, and frequency, GJO can significantly enhance the performance of WPT systems, ensuring efficient power transfer even in the presence of varying output power levels. The key strengths of GJO include:

- **Global Search Capability:** The exploration component of the algorithm allows it to search across a wide solution space, increasing the likelihood of finding the optimal solution.
 - **Local Search Refinement:** Through the exploitation phase, GJO can fine-tune solutions based on previously found good areas of the search space, improving the efficiency of the optimization.
- Simplicity and Flexibility: The algorithm is easy to implement and adaptable to various optimization problems across different domains.

By incorporating the Golden Jackal Optimization algorithm, it is possible to address the challenges associated with power loss in WPT systems, optimize energy transfer efficiency, and enhance overall system performance. GJO's ability to intelligently balance exploration and exploitation makes it an ideal tool for solving complex, real-world optimization problems, particularly in fields like electrical engineering, robotics, and systems design.

REFERENCES

- [1]. Rotenberg, Samuel A., Symon K. Podilchak, Pascual D. Hilario Re, Carolina Mateo-Segura, George Goussetis, and Jaesup Lee. "Efficient rectifier for wireless power transmission systems." *IEEE Transactions on Microwave Theory and Techniques* 68, no. 5 (2020): 1921-1932.
- [2]. Ngo, Tung, An-Dong Huang, and Yong-Xin Guo. "Analysis and design of a reconfigurable rectifier circuit for wireless power transfer." *IEEE Transactions on Industrial Electronics* 66, no. 9 (2018): 7089-7098.
- [3]. Liu, Xin, Fei Gao, Tianfeng Wang, Muhammad Mansoor Khan, Yun Zhang, Yue Xia, and Patrick Wheeler. "A multi-inverter multi-rectifier wireless power transfer system for charging stations with power loss optimized control." *IEEE Transactions on Power Electronics* 38, no. 8 (2023): 9261-9277.
- [4]. Sun, Jingdong, Jonghyun Cho, Anfeng Huang, Hongseok Kim, and Jun Fan. "Accurate rectifier characterization and improved modeling of constant power load wireless power transfer systems." *IEEE Transactions on Power Electronics* 35, no. 8 (2019): 7840-7852.
- [5]. Ozalevli, Erhan, Nicola Femia, Giulia Di Capua, Rajaram Subramonian, Dingkun Du, Joseph Sankman, and Mustapha El Markhi. "A cost-effective adaptive rectifier for low power loosely coupled wireless power transfer systems." *IEEE Transactions on Circuits and Systems I: Regular Papers* 65, no. 7 (2017): 2318-2329.
- [6]. Colak, Kerim, Erdem Asa, Mariusz Bojarski, Dariusz Czarkowski, and Omer C. Onar. "A novel phase-shift control of semibridgeless active rectifier for wireless power transfer." *IEEE Transactions on Power Electronics* 30, no. 11 (2015): 6288-6297.
- [7]. Li, Xing, Chi-Ying Tsui, and Wing-Hung Ki. "A 13.56 MHz wireless power transfer system with reconfigurable resonant regulating rectifier and wireless power control for implantable medical devices." *IEEE Journal of Solid-State Circuits* 50, no. 4 (2015): 978-989.
- [8]. Cheng, Bing, Liangzong He, Le Li, Houxuan Liu, and Fengwang Lu. "Improved wireless power transfer system utilizing a rectifier with nonlinear resistance compression characteristic." *Applied Energy* 331 (2023): 120365.
- [9]. Lu, Yan, Mo Huang, Lin Cheng, Wing-Hung Ki, and Rui P. Martins. "A dual-output wireless power transfer system with active rectifier and three-level operation." *IEEE Transactions on Power Electronics* 32, no. 2 (2016): 927-930.